JOURNAL OF MASS SPECTROMETRY, VOL. 32, 1151–1161 (1997)

SPECIAL FEATURE: TUTORIAL

Coincidence Measurements in Mass Spectrometry

M. J. Van Stipdonk,* E. A Schweikert† and M. A. Park‡
Center for Chemical Characterization and Analysis, Texas A&M University, College Station, Texas 77843-3144, USA

The detection of coincidental emissions (electron–ion, ion–ion, photon–ion) can enhance the amount of information available in desorption time-of-flight mass spectrometry (TOF-MS) by identifying physical, chemical and/or spatial correlations. This paper outlines the conditions for coincidence measurements and the methodology for identifying correlations. Applications of coincidence–correlation mass spectrometry include the study of the composition and structure of polyatomic ions, the process involved in ion production from solids and the chemical microhomogeneity of surfaces. © **1997 John Wiley & Sons, Ltd.**

J. Mass Spectrom. **32**, 1151–1161 (1997)
No. of Figs: 12 No. of Tables: 0 No. of Refs: 18

KEYWORDS: coincidence measurements; polyatomic ions; ion production from solids; microhomogeneity of surfaces

INTRODUCTION

The detection of coincidental signals is a well established practice in nuclear science.[1] One advantage of 'coincidence counting' is that it enhances the selectivity and hence the accuracy of the measurement. For instance, radioisotopes decaying via positron emission can be selectively identified and localized (in the case of positron emission tomography) by detecting the two coincidental γ-rays resulting from positron annihilation. This example refers to signals coincidental in time. More generally coincidental detection can be applied to signals that originate from a single event. This concept is the basis of time-of-flight mass spectrometry (TOF-MS), which is a record of congeneric events.

In TOF-MS, the mass spectrum is a histogram of abundances of temporally dispersed ions produced by the repeated application of a pulsed source of primary excitation. The primary pulse might come in the form of MeV energy heavy ions (plasma desorption mass spectrometry, (PDMS)), keV atoms or ions (fast atom bombardment, (FAB)), secondary ion mass spectrometry (SIMS) or IR or UV wavelength photons (matrix-assisted laser desorption ionization, (MALDI)). The secondary ion mass spectrum is a collection of coincidence events: each secondary ion originates from and hence is in (delayed) coincidence with the primary excitation pulse. Often the interaction of the primary probe will stimulate the emission of multiple secondary signals, including secondary electrons and photons in addition to the secondary ions. Two or more of these secondary signals detected together are in coincidence with each other as well as with the excitation pulse.

In this paper, we discuss the methodology and application of coincidence measurements in desorption/ionization mass spectrometry. One application is to determine the number of desorbed ions per incident bombarding particle. Such measurements are key for studying the 'cluster effect,' i.e. for the quantitative assessment of the enhanced secondary ion yields obtained with cluster projectiles in comparison with single atom impact.[2] Coincidence counting can also be used to correlate the emission of ionized and neutral fragments from the metastable dissociation of single precursor ions or to search for the correlated emission of secondary ions from the same initiating excitation pulse. The latter can reveal spatial and chemical relationships.

As noted already, schemes for detecting coincidental emissions and identifying correlations are commonly used in nuclear physics and chemistry. In desorption/ionization mass spectrometry, coincidence measurements have been practised by only a few groups. This is mainly due to certain prerequisites. First, the primary excitation pulses must be discrete and identical. Second, the detection system must be able to detect individual secondary ions, electrons and/or photons and only a few of these signals should occur per excitation pulse. The latter requirement is difficult to meet in conventional mass spectrometric techniques such as MALDI or electrospray; indeed, secondary ion multiplicity (simultaneous emission of identical secondary ions) must be negligible for the application of coincidence methods. Hence the approach used in coincidence mass spectrometry is to bombard a solid surface with individual primary ions (keV mono- and polyatomic and MeV heavy ions), each resolved in time and space. Each impact in turn is coupled with secondary ion, photon and electron detection at the single event level.

* Present address: Ionwerks, 2472 Bolsover Suite 225, Houston, Texas 77055, USA.
† Correspondence to: Emile A Schweikert, Center for Chemical Characterization and Analysis, Texas A&M University, College Station, Texas 77843-3144, USA.
‡ Present address: Bruker Instruments, Inc., 19 Fortune Drive, Manning Park, Billerica, Massachusetts 01821, USA.
Contract grant sponsor: National Science Foundation.
Contract grant sponsor: Texas Advanced Technology Program.

CCC 1076–5174/97/111151–11 $17.50

Received 4 September 1997
Accepted 22 September 1997

ELECTRON–ION COINCIDENCE FOR YIELD MEASUREMENTS

Coincidence counting can be used to select specific desorption events in TOF secondary ion mass spectrometric experiments where the source of projectiles emits simultaneously several types of ions. Despite their complex output, sources of energetic clusters are of interest because they can significantly improve the yield of secondary ions, an attractive feature for SIMS applications.[2] We have constructed several simple dual TOF mass spectrometers that when combined with coincidence counting allow one to identify the secondary ions produced by different polyatomic ion impacts. The heart of the instrument is a fast, high timing resolution time-to-digital converter (TDC). Several instrument companies offer TDCs; those used in the studies described here were developed at the Institute de Physique Nucleaire, Orsay, France.[3]

Using appropriate source materials, suites of projectiles can be produced that have the same origin in time. For instance, our ion sources generally use ^{252}Cf fission fragments to create atomic and polyatomic ions that are accelerated and used as primary projectiles. The fission fragment impact (and the registration of the complementary fragment at a start detector) defines the origin in time. Each primary ion is allowed to impact the sample target; no mass selection step is used to sort the primary ions while in flight. By using the fission fragment start and secondary electrons produced by the projectile impact, a primary ion mass spectrum is collected. Without primary ion selection, the secondary ion spectrum is a composite of several overlapping mass spectra, each generated by a given primary ion. Examples of a primary ion and of a composite secondary ion spectrum are shown in Figs. 1 and 2, respectively. In Fig. 2 the secondary ion peaks are labeled with the primary ion causing its emission indicated in parenthetical subscripts. Since the primary ion and secondary ion spectra are collected in the event-by-event mode, coincidence counting can be used to deconvolute the composite spectrum. We have developed a software data acquisition system that allows the simultaneous recording of total or conventional (all secondary ions sputtered by all primary ions) mass spectra and a series of coincidence spectra (where a restriction is placed on those events saved to make up the mass spectrum, see below). Time windows are set using channel markers around the secondary electron peaks for each primary ion. When an electron is detected within a time window, usually set on either side of the electron peak at its intersection with the background, it is assumed that a particular primary ion has hit the sample. Each secondary ion detected in coincidence with that electron is recorded in a reserved space of computer memory. By summing these individual events, correlated electrons and ions produced by a single primary projectile impact, a coincidence spectrum is produced which is a complete mass spectrum of the ions produced by the impact of that primary ion. It is important to note that the total and coincidence spectra are composed of events that come from the same data stream out of the TDC: all spectra are acquired simultaneously. Figure 3 shows a deconvoluted spectrum produced by selecting only those secondary ions emitted by the impact of one primary projectile. With the individual secondary spectra, it is possible to measure the secondary ion yields due to different primary projectiles in a single experiment. This procedure provides ready data for comparison because the experimental conditions (target surface conditions, transmission efficiencies and detec-

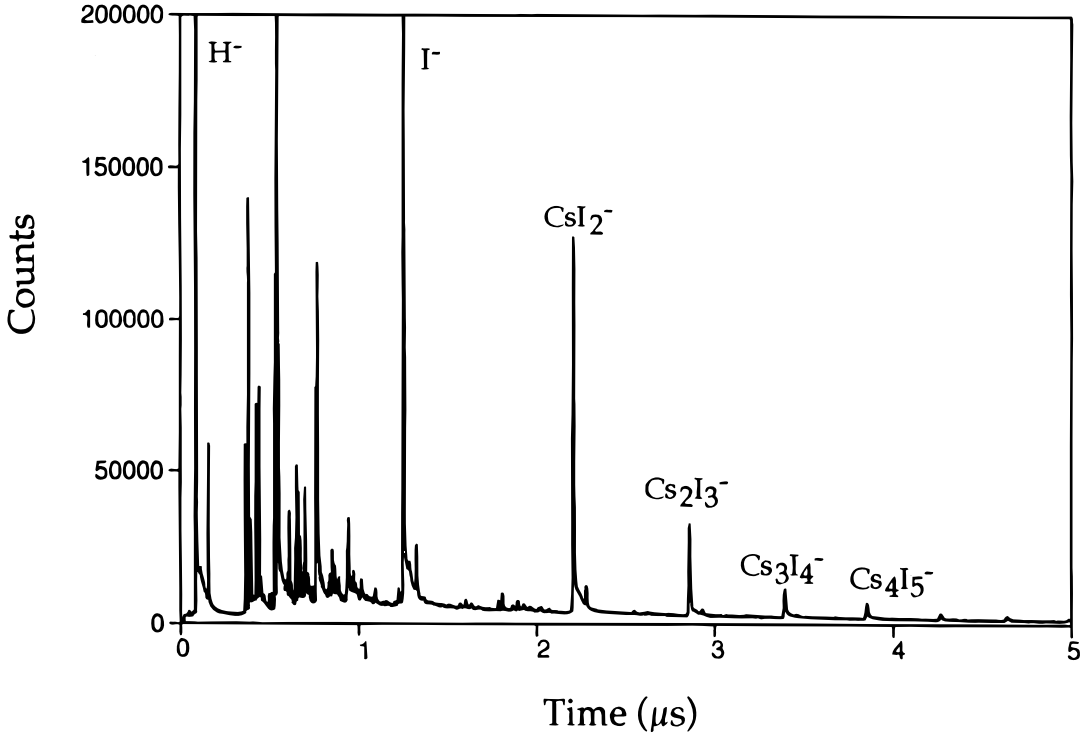

Figure 1. Suite of primary ions obtained from a CsI source and accelerated to 27 keV.

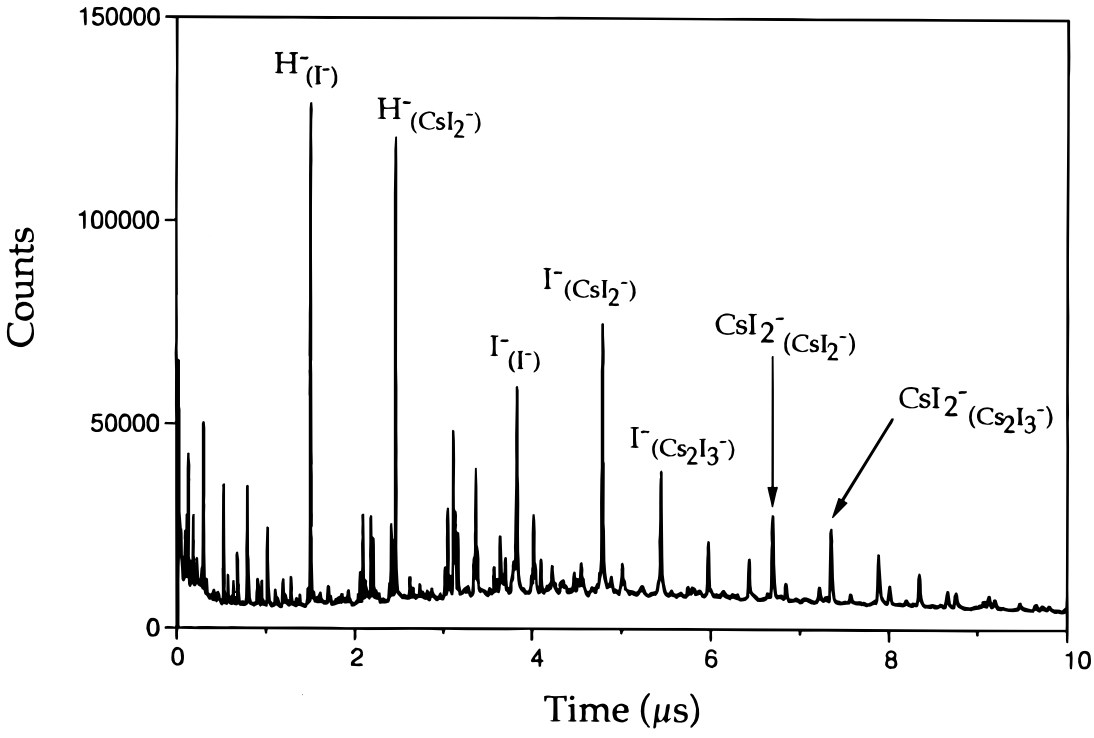

Figure 2. Secondary ion spectrum produced when the sequence of 27 keV primary ions (I^-, CsI_2^-, $Cs_2I_3^-$ shown in Fig. 1) bombards a CsI target.

tion efficiency) are the same. From these types of measurements we have determined that complex, polyatomic primary ions are more efficient on a per projectile basis for sputtering secondary ions than atomic primary ions at either the same impact energy or velocity. Such measurements, and also the physical and chemical effects of polyatomic projectile impacts at keV energies, remain a continuing theme of our research and of work in other laboratories.[4–8]

If a photomultiplier tube (PMT) is placed in line of sight with the sample target in a similar experimental arrangement, coincidental emission of electrons, ions

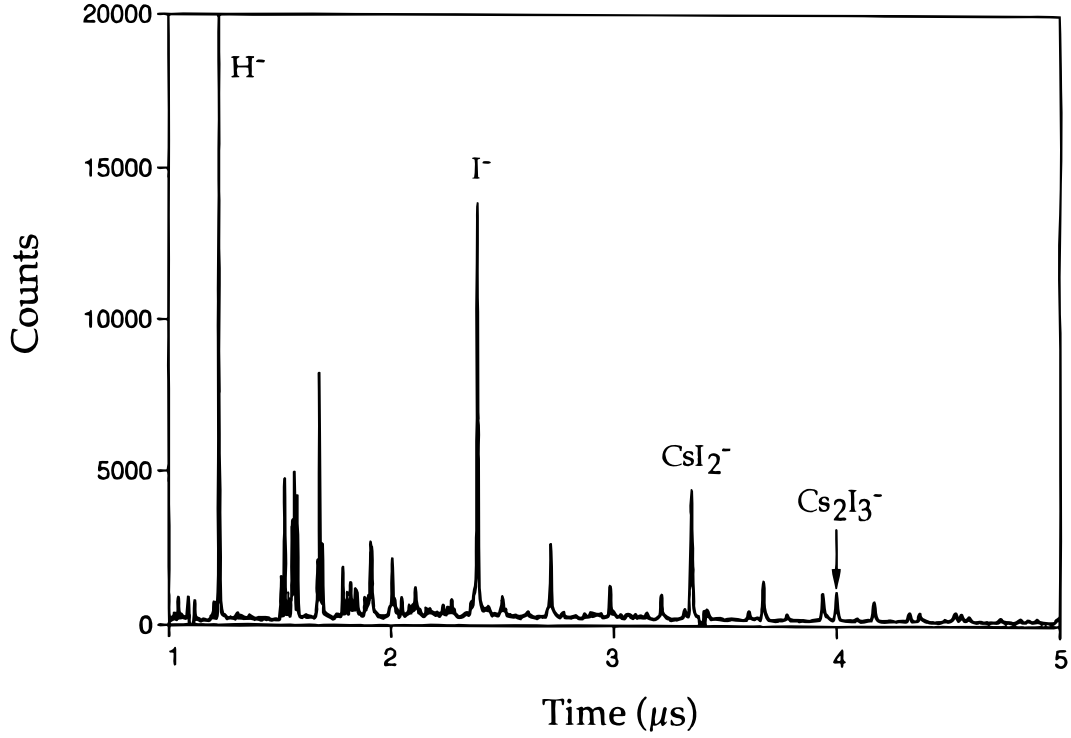

Figure 3. Secondary ion spectrum due to the impact of 27 keV CsI_2^- projectiles on CsI. This spectrum is deconvoluted from that shown in Fig. 2.

and photons can be measured. Using such a set-up, we have measured the photon emission stimulated by single atomic and polyatomic projectile impacts at room temperature. By using the coincidental emission of secondary electrons (to register the impact of a particular primary ion) and secondary photons, the number of photons emitted per projectile impact, and also their wavelength and fluorescence lifetimes, have been measured.

ION–NEUTRAL AND ION–ION COINCIDENCES

In mass spectrometric techniques such as MALDI, PDMS and SIMS, the mass spectra are recorded in the event-by-event mode. This means that the results of a single excitation pulse are analyzed before a subsequent pulse is addressed. For the case of ion impacts, statistically meaningful data sets are produced by summing a large number ($>10^6$) of primary events. Because PDMS uses individual MeV energy ions as the excitation probe, it is well suited for the application of coincidence counting to study the coincidental emission and possible correlation of secondary ions.

The same TDC and acquisition software as used for the secondary ion yield measurements are applied to perform ion–neutral or ion–ion coincidence measurements. Instead of setting time windows on secondary electrons, as is the case in the yield measurements, the windows can be placed on secondary ions of interest. Thus coincidence spectra are obtained by recording the results of those primary ion impacts which caused the emission of a selected primary ion. Thus, say, an Na^+ coincidence spectrum would be produced from the results of only those primary projectile hits from which an Na^+ ion was observed. To determine when an ion of interest has been detected, a flight time window is set around the peak of interest, e.g. Na^+. It is assumed that if a signal is detected at a flight time falling within the window, the ion of interest has been detected. A series of windows can be set sequentially throughout the conventional TOF mass spectrum. The coincidence spectra can be recorded and displayed in the form of a two-dimensional (2-D) matrix.[9] A 2-D TOF mass spectrum of NaF crystals on a polystyrene film is shown in Fig. 4.

Correlation coefficients

The rationale for acquiring coincidence spectra is to identify physical and/or chemical correlations or anti-correlations. Anticorrelations between ions implies that the likelihood of desorption of one of the ions is reduced when the other ion is desorbed. The question then is to quantify correlation. Two methods have been developed—that of a correlation coefficient and that of percentage coincidence.[10] If we assume that the desorption of ion A^+ is independent of the desorption of B^+ and vice versa, then the probability of observing ion A^+ and B^+ from the same impact, $P(A^+, B^+)$, should equal the product of the probability of observing ion A^+ due to a given primary ion impact, $P(A^+)$, and that of observing ion B^+ from a primary ion impact, $P(B^+)$. If the observed probability $P(A^+, B^+)$ is significantly greater than the expected probability, $P(A^+)P(B^+)$, then one may conclude that ions A^+ and B^+ are correlated.

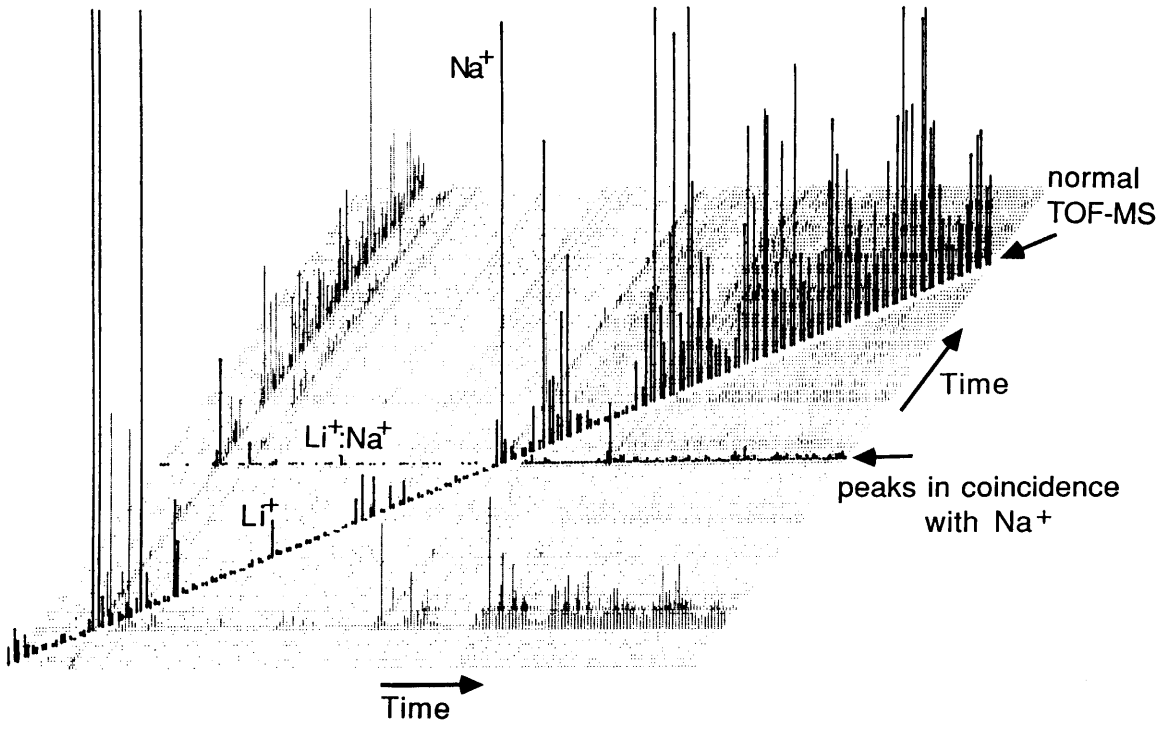

Figure 4. A portion of the two-dimensional spectrum of about 0.5 μm diameter NaF crystals on a spin-cast polystyrene film. The 'normal' spectrum along the diagonal and the Na^+ coincidence spectrum have been highlighted. (Reprinted with permission from M. A. Park, K. A. Gibson, L. Quiñones and E. A. Schweikert, *Science* **248**, 988 (1990). Copyright 1990 American Association for the Advancement of Science.)

To quantify the correlation better, we have defined a correlation coefficient and a percentage coincidence. The correlation coefficient is given by

$$Q = P(A^+, B^+)/[P(A^+)P(B^+)]$$

The probability of a given event occurring is determined experimentally by dividing the number of times that event is observed by the number of measurements taken. The experimental probability of observation of ion A^+ from a given primary ion impact is thus given by

$$P(A^+) = N(A^+)/S$$

where $N(A^+)$ is the number of counts in peak A^+ and S is the number of primary ions striking the sample surface during the analysis period. The correlation coefficient can then be related to the observed data via the area in the secondary ion peaks in the conventional (total) and coincidence spectra:

$$\begin{aligned} Q &= P(A^+, B^+)/[P(A^+)P(B^+)] \\ &= [N(A^+, B^+)/S]/\{[N(A^+)/S][N(B^+)/S]\} \\ &= [N(A^+, B^+)S]/[N(A^+)N(B^+)] \end{aligned}$$

If $Q = 1$, then the ions are independent on one another. If $Q > 1$, then the ions are correlated, that is, the desorption of one is dependent on the desorption of the other in a positive way. If $Q < 1$, then the ions are anti-correlated. Note that Q assumes ion emission under conditions where the Poisson distribution applies. It is useful to plot the correlation versus mass of the secondary ions as shown in Fig. 5. The secondary ion mass refers to the mass of the secondary ions that are being related to H^+. There are three noteworthy features in this plot, the baseline at $Q = 1$ and the two sets of points above the baseline. The baseline indicates non-correlation, that is, most secondary ions are unrelated to the desorption of H^+.

The two sets of points that project above the baseline indicate that two sets of hydrocarbon ions (CH_m^+ and $C_2H_m^+$) are correlated with H^+ to varying degrees. As seen in the plot, the hydrocarbon species containing less hydrogen are more correlated with H^+. These trends suggest that the hydrocarbon ions and H^+ have a common spatial and chemical origin.

Calculation of percentage coincidence

The second method of quantifying the correlations between the secondary ions is via percentage coincidence. Percentage coincidence is defined as the percentage of a given peak observed in coincidence with a second peak. This is related to the data and the correlation coefficient discussed above as

$$\begin{aligned} \%(A^+, B^+) &= [N(A^+, B^+)/N(B^+)] \times 100 \\ &= \{[N(A^+, B^+)/S]/[N(B^+)/S]\} \times 100 \\ &= [P(A^+, B^+)/P(B^+)] \times 100 \\ &= QP(A^+) \times 100 \end{aligned}$$

where $\%(A^+, B^+)$ is the percentage coincidence of B^+ with A^+. Because $P(A^+)$ is constant for a given acquisition, $\%(A^+, B^+)$ is proportional to Q. Hence a higher percentage coincidence of an ion with A^+ implies a greater correlation of that ion with A^+. Such a percentage coincidence may also be plotted *vs.* the mass of the secondary ions.

Figure 6 is the plot of percentage coincidence with H^+ *vs.* the mass of secondary ions produced from a PET target. This plot shows the same features as the H^+ correlation plot in Fig. 5, but additional information can be obtained from the percentage coincidence of the baseline. Secondary ions that are independent of one another can still occur in coincidence with one another, but the coincidence should be random. Thus, if

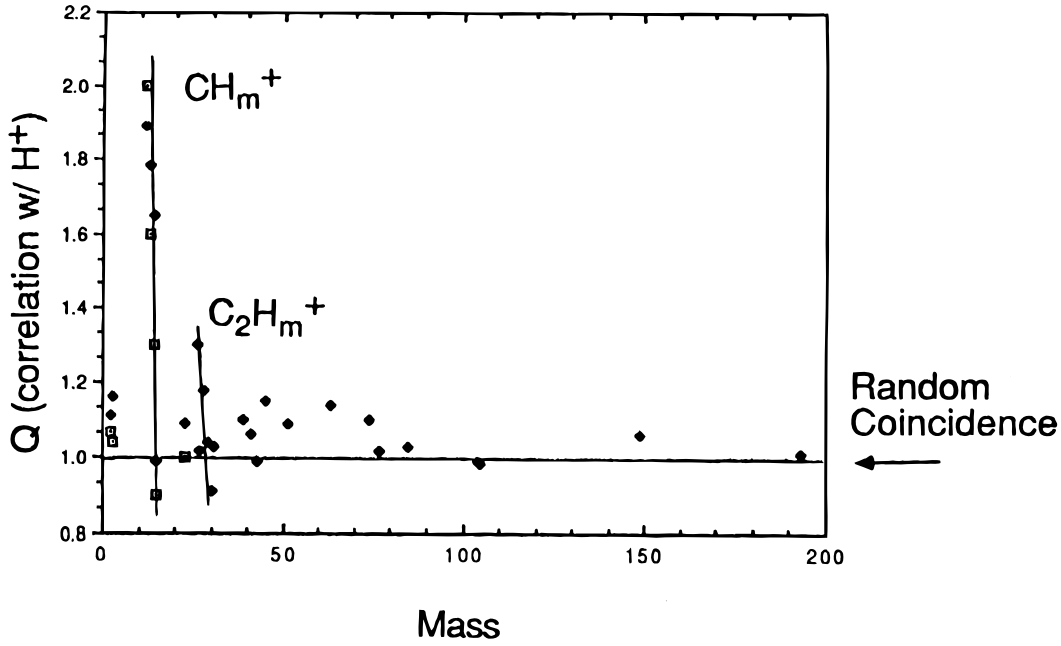

Figure 5. Correlation of emission of secondary ions with emission of H^+. Data are from a Cf-252 PDMS experiment on PET.[5] (From M. A. Park, PhD Dissertation, Texas A&M University (1991).)

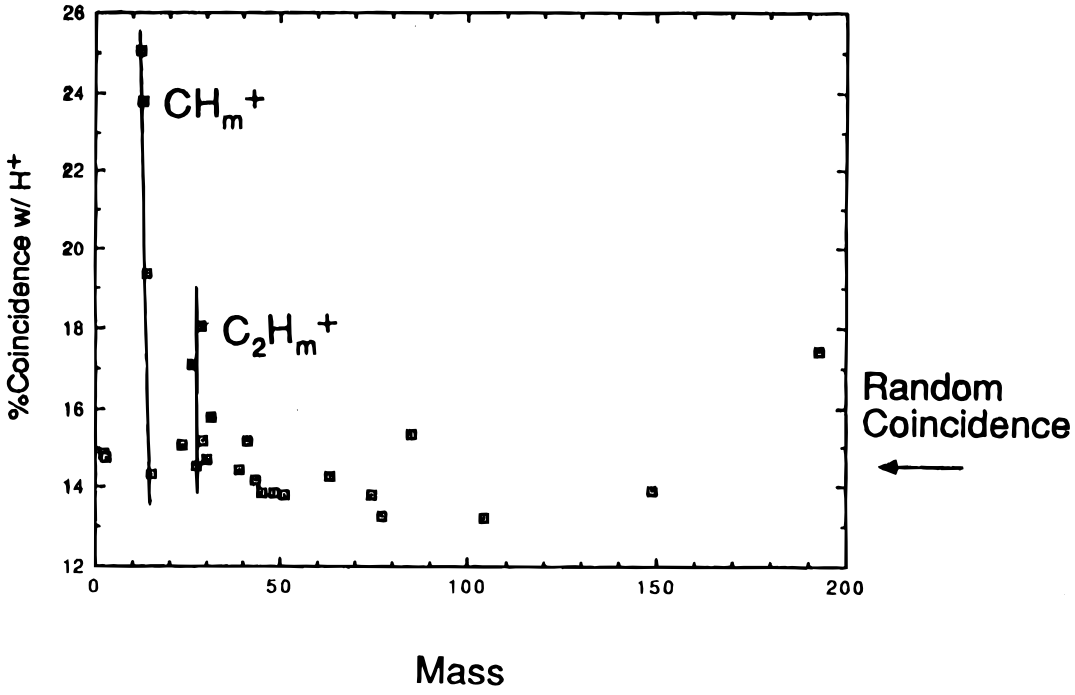

Figure 6. Same data as in Fig. 5, presented as percentage coincidence.[5] (From M. A. Park, PhD Dissertation, Texas A&M University (1991).)

A^+ and B^+ are independent in their emission and the percentage yield of A^+ is 15%, then 15% of those desorption events producing B^+ should also produce A^+. That is, when $Q = 1$,

$$\%(A^+, B^+) = QP(A^+) \times 100$$
$$= P(A^+) \times 100$$

Because the percentage yield of A^+, $\%Y(A^+)$ is defined as the percentage of ions that produce an A^+ ion, i.e. $P(A^+)$,

$$\%(A^+, B^+) = \%Y(A^+), \quad \text{if } Q = 1$$

Hence the percentage coincidence can be used to determine the percentage yield of secondary ions of interest.

Applications

Coincidence mass spectrometry relies on physical and chemical processes generating correlated signals. In

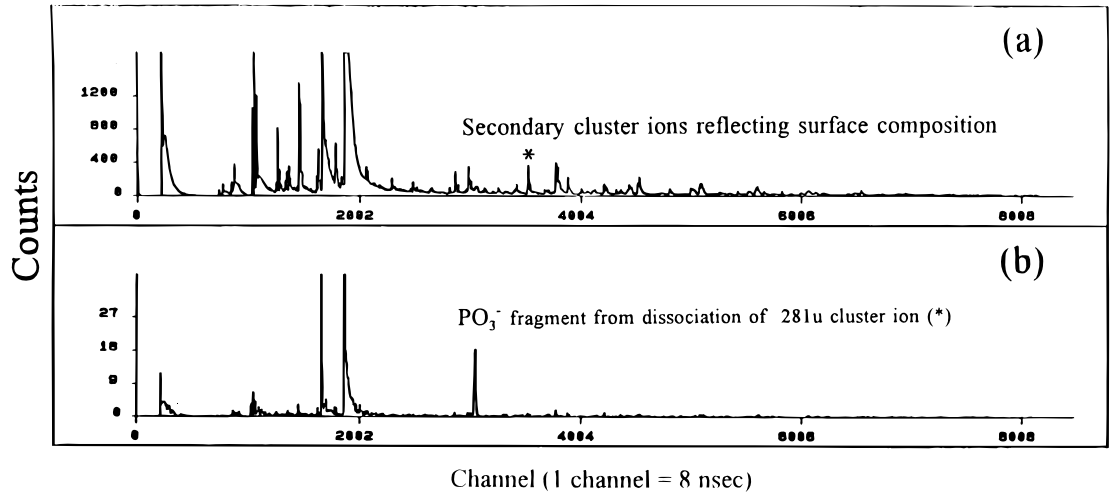

Figure 7. Comparison of reflected ion spectra. (a) Total reflected ion spectrum. The peak labeled with an asterisk is the 281 u precursor cluster ion monitored for metastable decay. (b) Reflected ions in coincidence with the neutral detected from the dissociation of the 281 u cluster ion. Other peaks in the spectrum are secondary ions in random coincidence with the detected neutral or due to secondary ion multiplicity effects. (Reprinted with permission from M. J. Van Stipdonk and E. A. Schweikert, *Nucl. Instrum. Methods Phys. Res. B* **112**, 68 (1996). Copyright Elsevier Science 1996.)

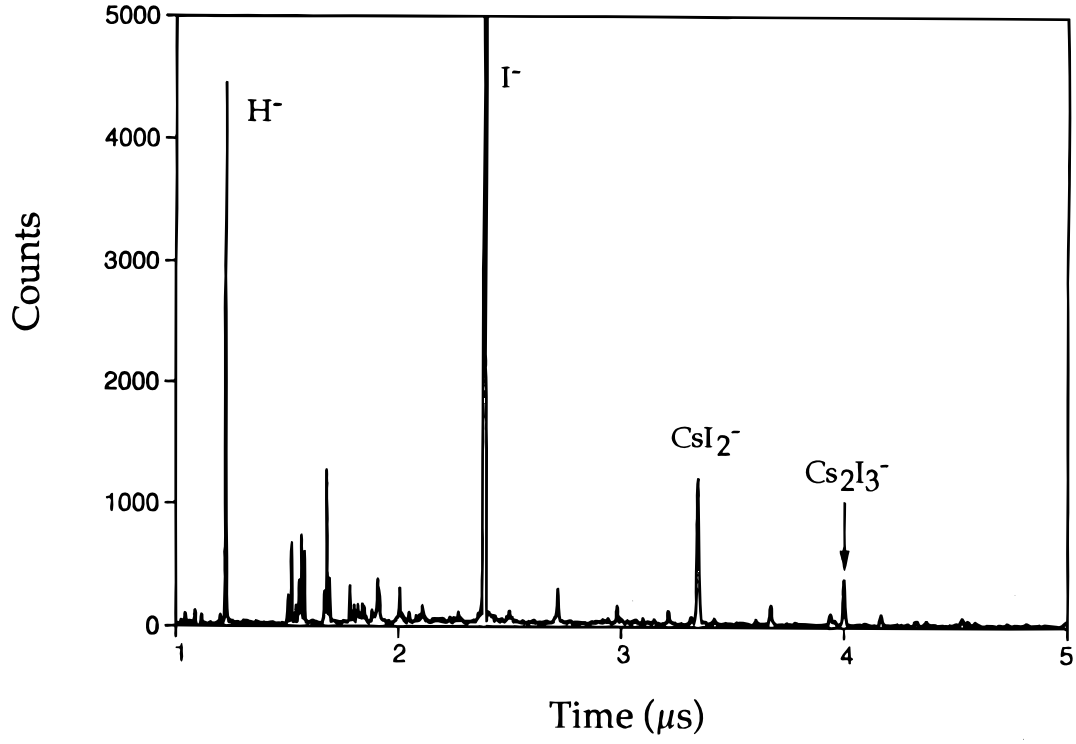

Figure 8. Coincidence spectrum of I^- with other secondary ions when CsI is bombarded with 27 keV CsI_2^-. (Adapted from K. B. Ray, PhD Dissertation, Texas A&M University (1994).)

practice, only those which can be observed experimentally as discrete events are of interest. We consider here applications based on the detection of two coincidental secondary ions (SIs) or an SI ion and neutral. If they originate from the same parent molecule we have a chemical correlation. The definition can be broadened to include cases where the starting material is an aggregate of like molecules from which two chemically related ejecta are formed. In most cases correlated signals have a common spatial origin, i.e. they are

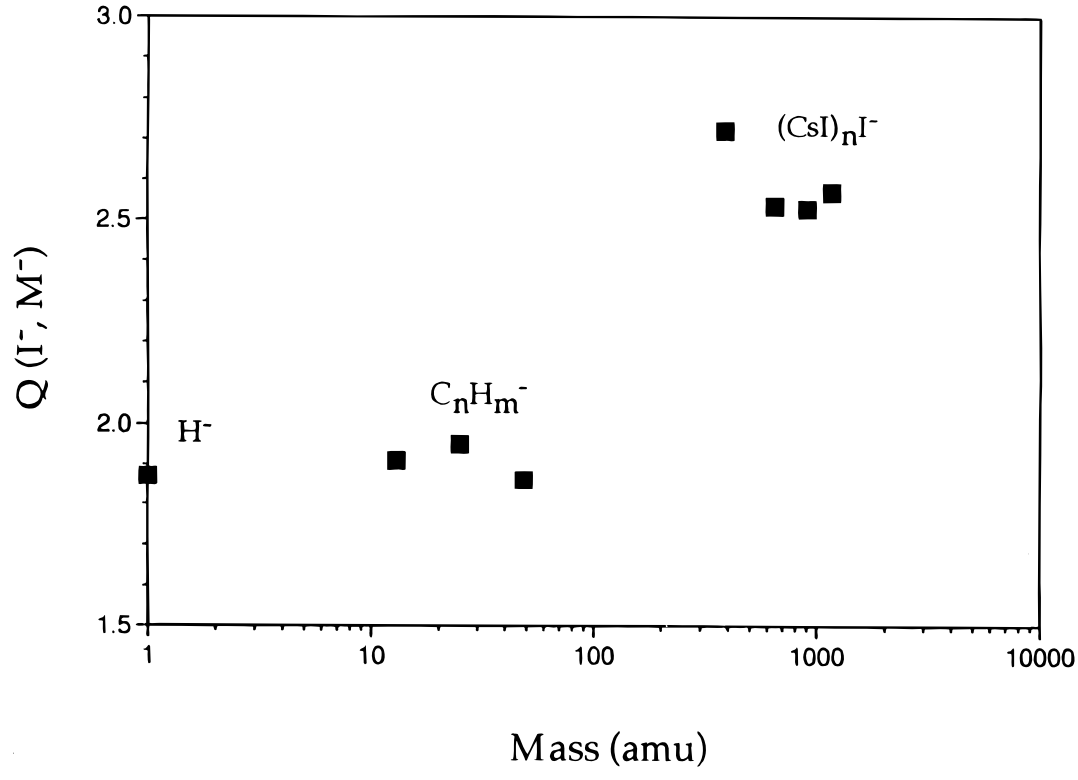

Figure 9. Plot of the correlation coefficient with I^- *vs.* the mass of the secondary ion of interest. (From K. B. Ray, PhD Dissertation, Texas A&M University (1994).)

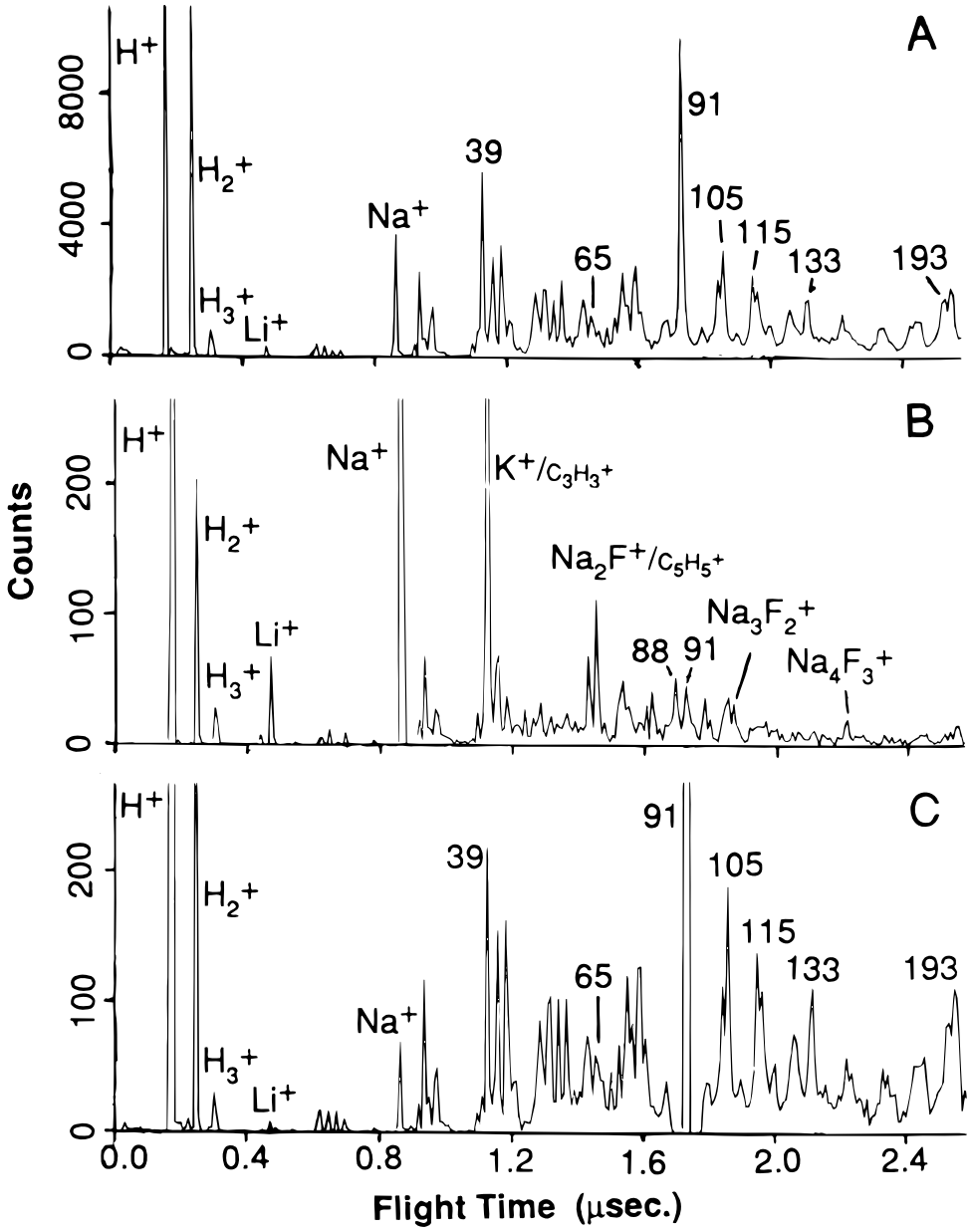

Figure 10. Mass spectrum of (A) NaF crystals on a polystyrene film; (B) and (C) are the coincidence spectra from the same sample for mass 23 (Na^+) and mass 91 (from PS), respectively. (Reprinted with permission from M. A. Park, K. A. Gibson, L. Quiñones and E. A. Schweikert, *Science* **248**, 988 (1990). Copyright 1990 American Association for the Advancement of Science.)

emitted from the same desorption site. No chemical relationship is implied here, but the nanometric dimensions of the desorption site mean that correlated ejecta reflect microhomogeneity.

The model case for chemical correlation is unimolecular decay, where a polyatomic ejecta dissociates into an ionized and neutral fragment. The ion–neutral coincidences can be studied at the single event level of a TOF mass spectrometer equipped with an electrostatic mirror or mass reflectron. The methodology was pioneered by Della-Negra and Le Beyec.[11] An illustration of the data obtained from metastable polyatomic ejecta is presented in Fig. 7. This case relates to species desorbed from α-phase zirconium phosphate (αZrP) under ^{252}Cf fission fragment impact (plasma desorption).[12] Intact ions along with the ionic fragments are reflected by the electrostatic mirror into a detector, while the neutrals are unaffected by the electrostatic field and pass through the reflectron to strike another detector. Figure 7(a) shows the reflected ion spectrum. It can be compared with the spectrum in Fig. 7(b), showing the reflected ions in coincidence with a selected neutral fragment. This example indicates that αZrP clusters decompose by ejection of PO_3^- group. Ion–neutral correlations can provide insight into the composition and structure of cluster ions and back to that of the original solid. It is important to note that such ion–neutral coincidences are absolutely correlated and offer an opportunity for the accurate identification of very small numbers of molecular species. The implicit assumption is that there is no ambiguity in the chemical identity of the ionized and neutral fragments. If this assumption is met, the absolute ion–neutral correlation might allow the identification of a single molecule with

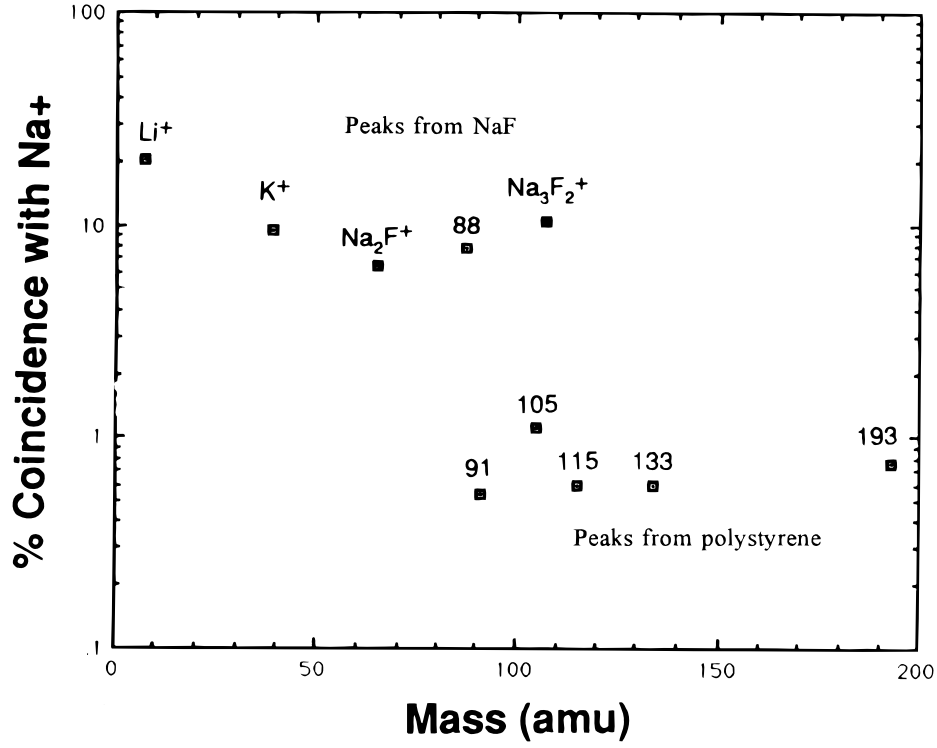

Figure 11. Plot of percentage coincidence with Na^+ coincidence *vs.* mass. The set of points with high percentage coincidence represent peaks associated with NaF, and those points with low percentage coincidence are associated with PS. (Reprinted with permission from M. A. Park, K. A. Gibson, L. Quiñones and E. A. Schweikert, *Science* **248**, 988 (1900). Copyright 1990 American Association for the Advancement of Science.)

high accuracy. In principle, detection of a single molecule could be achieved with 99% certainty based on the observation of the correlated signals from an average of five molecules. The ion–neutral concept should also be applicable to the products of collision-induced dissociation.[13]

The examination of SI emission as a function of the primary ion characteristics or 'entrance' conditions can be extended to revealing SI emission as a function of 'exit' conditions, specifically the conditions for coincidental emissions of SIs. We are not considering here coincidental SIs from the same parent molecule, but SIs from the same desorption event and hence the same site. Hence the experiment is to determine via coincidence counting if the emission of a specified SI is correlated with another SI. Consider the mass spectrum shown in Fig. 3. The intense peak due to I^- emission is a frequent occurrence. We can now ask: which SIs are emitted coincidentally with I^- when CsI_2^- projectiles bombard CsI? The resulting mass spectrum is shown in Fig. 8. The coincidence counts can be tested for correlation by calculating correlation coefficients, Q, for I^- with various SIs (Fig. 9). Clearly there is a strong correlation between I^- and $(CsI)_nI^-$, pointing to a relationship between these ions desorbed from CsI. The significance of this correlation is discussed elsewhere.[14] Briefly, SIs may be related to one another because they originate from preformed aggregations.

It was suggested some time ago that secondary ions emitted in coincidence due to spatial correlation could be used to test for chemical microhomogeneity.[15] The approach, as in previous examples, relies on event-by-event bombardment of a surface with keV or MeV energy ions. A single projectile addresses only a small region of the surface, the secondary ions are emitted from a spot ~10 nm in diameter.[16] If the surface is heterogeneous on a scale larger than the size of the desorption site, a given projectile would ideally reveal only one chemical compound per impact. In such a case, secondary ions from different compounds would not frequently be desorbed together from the same projectile impact. Alternatively, if a sample surface has multiple components mixed homogeneously (relative to the size of the desorption site), then a single primary ion may generate simultaneously secondary ions from multiple chemical compounds within the desorption site. Hence the ability to detect the homogeneity of a surface via coincidence counting depends on the size of the spatial segregation of compounds on a surface in relation to the size of the desorption site. The latter should be as small as possible to maximize spatial resolution. This condition is readily met in the case of spatially and temporally resolved single projectile impacts. An additional requirement for the successful application of the micro-homogeneity test is that each sample compound must produce a distinct mass spectral peak, so that individual components can be distinguished from one another.[17]

The ability to discern spatial segregations is illustrated with the example of analyzing small NaF crystals (~0.5 mm in diameter) dispersed on a polystyrene (PS) film (~3% surface coverage). Figure 10 shows three spectra acquired simultaneously. The conventional TOF spectrum contains peaks due to PS (m/z 91) and NaF (Fig. 10(A)). Figure 10(B) represents the secondary

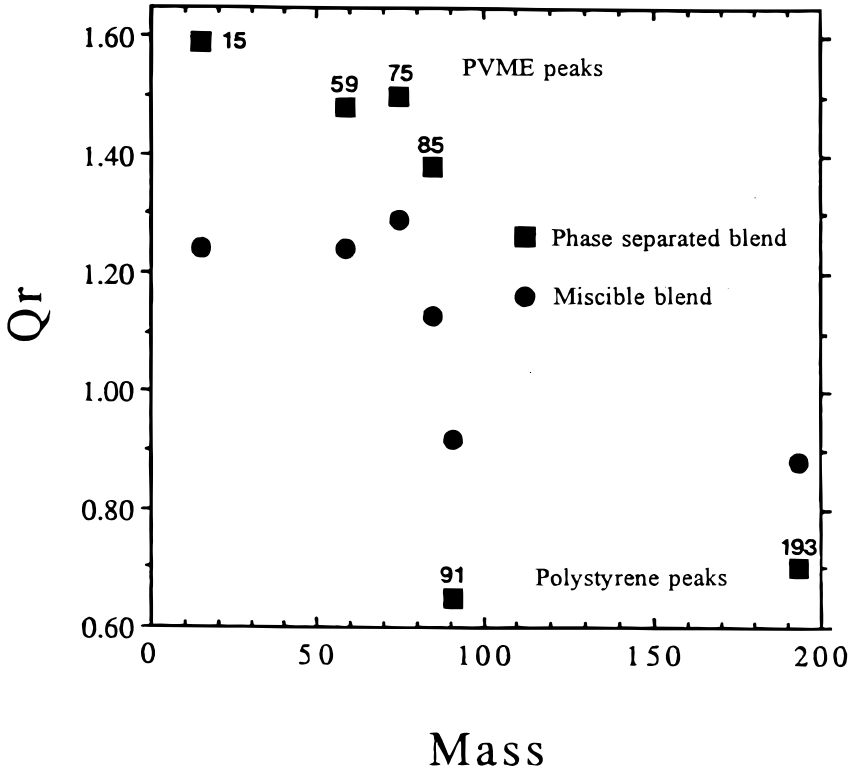

Figure 12. Plot of the correlation coefficient relative to mass 101 *vs.* secondary ion mass. Phase-separated (■) and miscible (●) data were taken from the analysis of 75:25 PS–PVME blends. (Reprinted with permission from B. D. Cox, M. A. Park, R. G. Kaercher and E. A. Schweikert, *Anal. Chem.* **64**, 843 (1992). Copyright 1992 American Chemical Society.)

ions in coincidence with m/z 23, Na^+, and is similar to a mass spectrum obtained from an NaF standard. Figure 10(C) is the mass 91 coincidence spectrum (a spectrum containing those primary ion impact events that include the detection of m/z 91), which strongly resembles the mass spectrum of a PS standard. There are significant differences between the spectra in Fig. 10(A) and (B), because the NaF is spatially segregated from PS. A simple test for identifying inhomogeneities is to plot the percentage coincidence (Fig. 11). A quantitative model for a more rigorous assessment of homogeneity has been discussed elsewhere.[17] The preceding example demonstrates the feasibility of analyzing surfaces for chemical homogeneity at the 100 nm level. The ultimate resolution limit of coincidence MS remains to be explored. A critical factor will be the perimeter of the segregation.

Another illustration of the coincidence–correlation procedure deals with the surface homogeneity of polymer blends.[18] The case studied dealt with miscible and phase separated blends of PS and polymethyl vinyl ether (PVME). Figure 12 is a plot of the correlation coefficient derived for various secondary ions with m/z 101 (a characteristic secondary ion emitted from PVME). The data shown in Fig. 12 are from two samples, one a miscible blend and the other a phase separated blend, both containing PS and PVME in a 75:25 mass ratio. The characteristic peaks of PS (m/z 91 and 193) show the largest degree of segregation ($Q \neq 1$) in the phase-separated sample. The Q values are closer to unity in the miscible sample (Q should be unity in a perfectly homogeneous blend). This example illustrates how mass spectrometry can be used to provide information that is difficult to obtain, namely the miscibility of a polymer blend at the surface, simply by paying attention to the coincidental emission of secondary ions from individual primary ion events.

CONCLUSION

Coincidence counting enhances the amount of information available from TOF-MS, viz. the composition and structure of polyatomic ions, the processes involved in secondary ion production and the chemical microhomogeneity of surfaces. The key feature of TOF-MS combined with coincidence counting is that it can reveal physical and/or chemical correlations from small numbers of atoms or molecules. The implications for chemical analysis remain to be fully explored. In particular, accurate assays should be feasible at the limits of analysis provided unambiguous correlated signals can be detected.

Acknowledgements

Work on coincidence counting mass spectrometry has been in progress for some years. It is a distinct pleasure to acknowledge the key contributions of K. A. Gibson, K. B. Ray and E. F. da Silveira and the financial support of the National Science Foundation and the Texas Advanced Technology Program.

REFERENCES

1. G. F. Knoll, *Radiation Detection and Measurement*, 2nd edn. Wiley, New York (1989).
2. M. G. Blain, S. Della-Negra, H. Joret, Y. Le Beyec and E. A. Schweikert, *Phys. Rev. Lett.* **63**, 1625 (1989).
3. E. Festa, R. Sellem and L. Tassan-Got, *Nucl. Instrum. Methods A*, **234**, 305 (1985).
4. J. C. Ingram, G. S. Groenewold, A. D. Appelhans, J. E. Delmore and D. A. Dahl, *Anal. Chem.* **67**, 165 (1995).
5. K. Boussofiane-Baudin, G. Bolbach, A. Brunelle, S. Della-Negra, P. Hakansson and Y. Le Beyec, *Nucl. Instrum. Methods B*, **88**, 160 (1994).
6. P. A. Demirev, J. Eriksson, R. A. Zubarev, P. Papaleo, G. Brinkman, P. Hakansson and B. U. R. Sundqvist, *Nucl. Instrum. Methods B*, **88**, 139 (1994).
7. J. F. Mahoney, J. Perel, S. A. Ruatta, P. A. Martino, S. Husain and T. D. Lee, *Rapid Commun. Mass Spectrom.* **5**, 441 (1991).
8. D. Fabris, Z. Wu and C. C. Feaselau, *J. Mass Spectrom.* **30**, 140 (1995).
9. M. A. Park, K. A. Gibson, L. Quinones and E. A. Schweikert, *Science* **248**, 988 (1990).
10. M. A. Park, PhD Dissertation, Texas A&M University (1991).
11. S. Della-Negra and Y. Le Beyec, *Anal. Chem.* **57**, 2035 (1985).
12. M. J. Van Stipdonk and E. A. Schweikert, *Nucl. Instrum. Methods B*, **112**, 68 (1996).
13. R. G. Cooks, personal communication (1997).
14. K. B. Ray, M. A. Park and E. A. Schweikert, *Nucl. Instrum. Methods Phys. Res. B*, **82**, 317 (1993).
15. S. Della-Negra, D. Jacquet, I. Lorthiois and Y. Le Beyec, *Int. J. Mass Spectrom. Ion Phys.* **53**, 215 (1983).
16. K. Wein, *Lect. Notes Phys.* **269**, 1 (1986).
17. K. B. Ray, M. A. Park, M. E. Inman and E. A. Schweikert, *J. Trace Microprobe Tech.* **10**, 91 (1992).
18. B. D. Cox, M. A. Park, R. G. Kaercher and E. A. Schweikert, *Anal. Chem.* **64**, 843 (1992).